
Master Thesis

- Implementation of stereo vision engine -

Project Report
Group 1072

Aalborg University
Electronics and IT

Copyright © Aalborg University 2015

Here you can write something about which tools and software you have used for typesetting the document, running simulations and creating figures. If you do not know what to write, either leave this page blank or have a look at the colophon in some of your books.??



Electronics and IT
Aalborg University
<http://www.aau.dk>

AALBORG UNIVERSITY
STUDENT REPORT

Title:

Stereo vision implementation??

Abstract:

Here is the abstract

Theme:

Master Thesis??

Project Period:

Spring Semester 2016

Project Group:

1072

Participant(s):

Tomas Brandt Trillingsgaard

Supervisor(s):

Peter Koch

Copies: 4

Page Numbers: 53

Date of Completion:

September 27, 2016

The content of this report is freely available, but publication (with reference) may only be pursued due to agreement with the author.

Contents

Preface	ix
1 Introduction	1
1.1 Stereo vision introduction	1
1.2 Motivation	2
1.3 Problem Introduction	2
1.4 Delimitation	2
1.5 Report Structure and Design Process	2
2 Application Analysis	5
2.1 The Basic Principal of Stereo Vision	5
2.2 Epipolar Geometry	8
2.3 Color space and grayscale	9
2.4 Disparity precision	10
2.5 Occlusions	13
2.5.1 Neighbor's Disparity Assignment (NDA)	14
2.5.2 Diffusion in Intensity Space (DIS)	15
2.5.3 Weighted Least Squares (WLS)	15
2.5.4 Segmentation-based Least Squares (SLS)	17
2.6 Occlusions filling result	18
2.7 Mini-conclusion	19
3 Requirements	21
3.1 Requirement specification	21
3.2 Test specification	22
4 Algorithm design	23
4.1 Efficient Edge Preserving Stereo Matching:	23
4.2 Fast Cost-Volume Matching:	24
4.2.1 Guided image filter	24
4.3 Simulation and comparison	25
4.4 Choosing an algorithm	25

5 Platform Analysis	27
6 Design methodology	29
7 Architecture design	33
7.1 Parallelism Analysis	33
7.2 Allocation and Scheduling	34
7.2.1 RC scheduling	35
7.2.2 TC schedule	37
7.3 Finite State Machine with Data Path design	37
7.3.1 FSMD example	37
7.4 VHDL + Simulation	40
8 Acceptance test	43
9 Conclusion	45
Bibliography	47
A Allocation test	49
A.1 General procedure	49
A.2 Adder	50
A.3 Subtract	50
A.4 Adder/Subtract	50
A.5 Multiplier - LUT	50
A.6 Multiplier - DSP48	51
A.7 Divider	51
B Extra Figures	53

Todo list

■ ROUGH SKETCH not done yet	23
■ simulation af de 2 algorithmer og samlign resultaterne.	25
■ Nok en anden titel til denne sektion. Skriv hvilken algoritme jeg går videre med	25
■ beskriv Zynq platformen. kom ind på hvad den indeholder	27
■ bedre navn og cite ds190 product specification og måske trm?	27
■ FPGA constraints ==> $C = f(A, T, P, N)$, Lav en tabel	27
■ læs om system design methodologies i gajski's Embedded Systems Design - Modeling, Synthesis and Verification og beskriv Platform Methodology	29
■ NOT DONE! rough sketch. De nedenstående trin er hvad jeg skal igen nem: Para. Anal., Alloc., Optimizaiton, FSMD og VHDL + simulering	33
■ lav om til operation og husk mult	35
■ find et bedre ord	37
■ tjek op på synkront dataflow diagram og state diagram	37
■ tænk i register! transfer! level og ikke i FSMD	37
■ udfør accept test udfra test specifikationen (brug data fra python simuler ing og giv det til VHDL implementationen)	43

Preface

Here is the preface. You should put your signatures at the end of the preface.

Aalborg University, September 27, 2016

Tomas Brandt Trillingsgaard
<ttrill10@student.aau.dk>

Chapter 1

Introduction

In this chapter, the project is introduced and motivated. Furthermore, a brief description is presented for stereo vision and the use for it at HSA systems. Lastly, this chapter also describes a delimitation of the project and report.

1.1 Stereo vision introduction

In 280 A.D the greek mathematician Euclid noticed that the perception of depth is caused by each eye receiving a dissimilar image of the same object. Throughout history different people have been working on this concept. In 1933 Sir Charles Wheatstone began mimic and forced the perception of depth by developing the stereoscope. The stereoscope use images taken by two cameras placed next to each other and the stereoscope then isolated the images so each eye only see one image. This mimics the depth perception and the viewer would be able to see depth in the images. [8]

Beginning around 1970 computer vision began appearing and a big part of this area is stereo vision, the measurement of depth mimicing the human vision using two cameras [7]. The ability to measure depths enables a computer to distinguish between objects and hence better interact and react on the world.

HSA systems wish to follow packages going through their system. A strategically placed stereo vision camera will enable them to know how many and where these packages are in the system. In case of errors and the like the printer system is the able to notice when the conveyor belt is empty and ready to reset.

In future uses HSA system would like the stereo vision system to have very precise depth measurements of ≤ 2 mm in the distances between 0.5-1.5 m.

1.2 Motivation

The area of stereo vision have been researched thoroughly and precise algorithms have been found but most algorithms are very heavy computational wise. HSA system wish for a stereo vision system which can run real-time (10 fps) and have a high precision of ≤ 2 mm between 0.5 m and 1.5.

1.3 Problem Introduction

HSA systems wish to follow packages going through their system. A strategically placed stereo vision camera will enable them to know how many and where these objects are in the system. The primary objectives of this is to:

- Analyze obstacles within stereo vision
- Analyze different stereo algorithms
- Design and optimize an architecture for executing stereo vision

1.4 Delimitation

This project is mainly concerned with the design and implementation of a hardware design for a FPGA. This project will not focus on developing a new stereo vision algorithm. Obstacles and issue with stereo algorithms will be analyzed but simpler solution will be used for most obstacles.

1.5 Report Structure and Design Process

The A³ model is a basic design model used internally at AAU and is illustrated on figure 1.1 on the facing page. The model consist of tree design domains which it will explore and it will help structure this report. These domains are Application, Algorithm and Architecture.

The search for a solution starts in the application domain where the problem and application are being explored. Chapter 2 on page 5: Application Analysis will explore the Application domain and the resulting specification for the application are presented in chapter 3 on page 21. In this project not a lot of applications are explored since the problem and the wanted application have been given by HSA system.

When moving to a new domain it can result in landing in different areas of the domain as seen on figure 1.1 on the next page. The solid arrows goes from a single

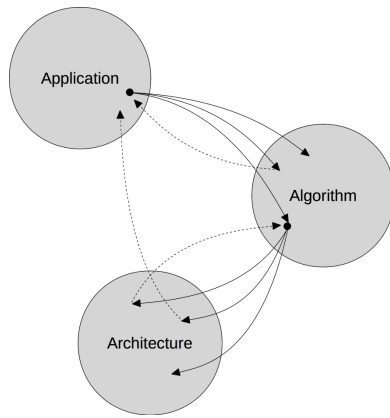


Figure 1.1: A³ model

point in the preceding domain and spreads out to different points in the current domain and these different points can, in the case of the algorithm domain, represent different algorithms. Chapter 4 on page 23 will explore the algorithm domain.

Chapter 6 on page 29 will described a methodology to go from a algorithm in the algorithm domain to some hardware architecture in the architecture domain.

Notice the dashed arrows in figure 1.1. These arrows shows that when you are exploring some domains new information might be given which require you to go back to a former domain and change the found specification etc. and then start moving to a new domain from new.

Chapter 8 on page 43 will test whether the found solution comply with the requirements in 3 on page 21 and chapter 9 on page 45 will conclude the project and its findings.

Chapter 2

Application Analysis

This chapter will explore the application domain from the A³ model. First, the basic principles of stereo vision will be described and then other aspects such as color versus grayscale etc. are analyzed. The results from this chapter will be used in the next chapter 3 on page 21.

2.1 The Basic Principal of Stereo Vision

A standard stereo vision setup consists of two similar cameras placed horizontally at a specified distance from each other. This distance is called the baseline. Figure 2.1 shows an example of this setup.

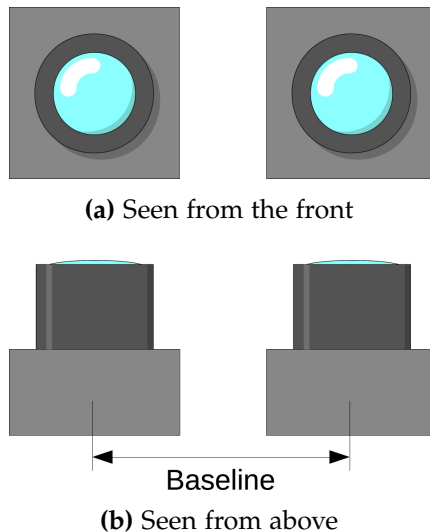


Figure 2.1: Illustration of a standard stereo setup

Figure 2.2 shows how a scene is seen by the camera, is inverted in the optical center and projected onto the image sensor in the camera. The original image plane is located at the position of the image sensor but it is inverted compared to the scene captured. To simplified comparisons to the real world, an image plane can be placed opposite of the optical center at the same distance from the center and this image plane will not be inverted.

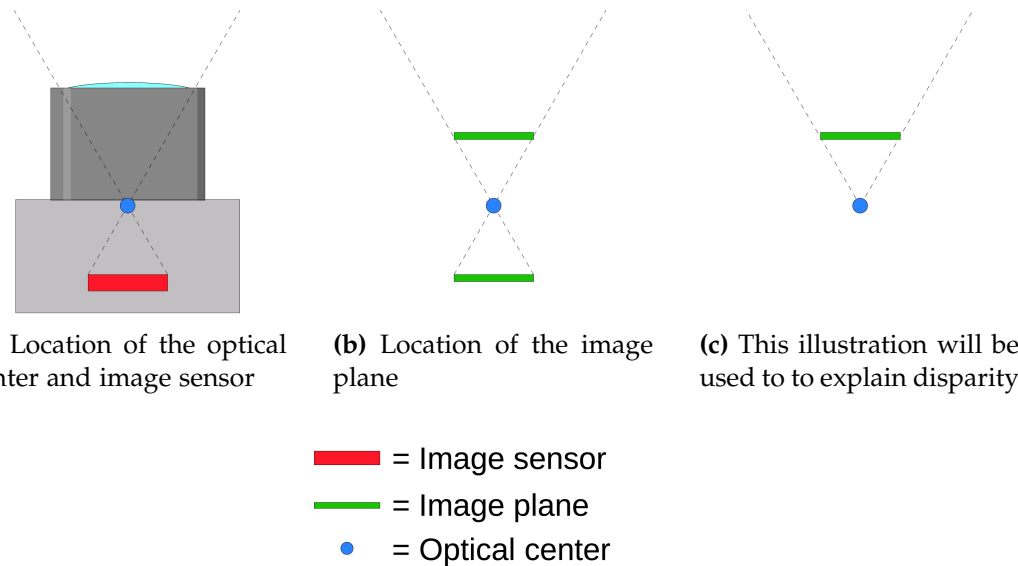


Figure 2.2: Illustration of going from camera to image plane

Figure 2.3a shows that a single camera is not able to differentiate between two points at the same angle from the optical center but a different distance. Figure 2.3b shows that adding the second camera shows that you then are able to differentiate between the two points.

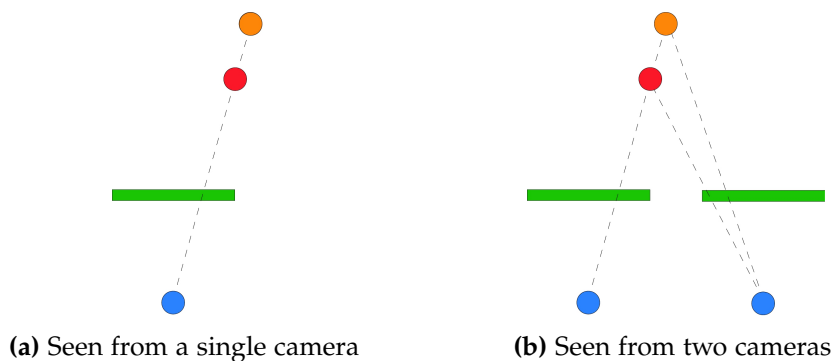


Figure 2.3: Example of two points in a scene at different depths

Figure 2.4 on the next page shows how the distance to a point can be calculated

from the difference in x-positions on the image plane (the disparity). Figure 2.4a and 2.4b shows how the disparity change depending on the distance to the point. Figure 2.4c shows the point in the scene (p), where line of sight cross the image planes (i_1 and i_2) and the optical centers (c_1 and c_2). From these points two similarly angled triangles can be created. One between p , i_1 and i_2 and the other triangle between p , c_1 and c_2 . For similarly angled triangles the ratio between the height and the bottom width is the same for each triangle and hence the following equation can be formed:

$$\frac{b}{z} = \frac{L}{z-f} = \frac{b - (x_1 - x_2)}{z - f} \quad (2.1)$$

$x_1 - x_2$ is also called the disparity, d , and equation 2.1 can be simplified:

$$z = \frac{b \cdot f}{d} \quad (2.2)$$

In equation 2.2 b and f is known hence only the disparity is needed to find z . So to find the distance to a point you should find the location of the point in the two images and calculate the displacement.

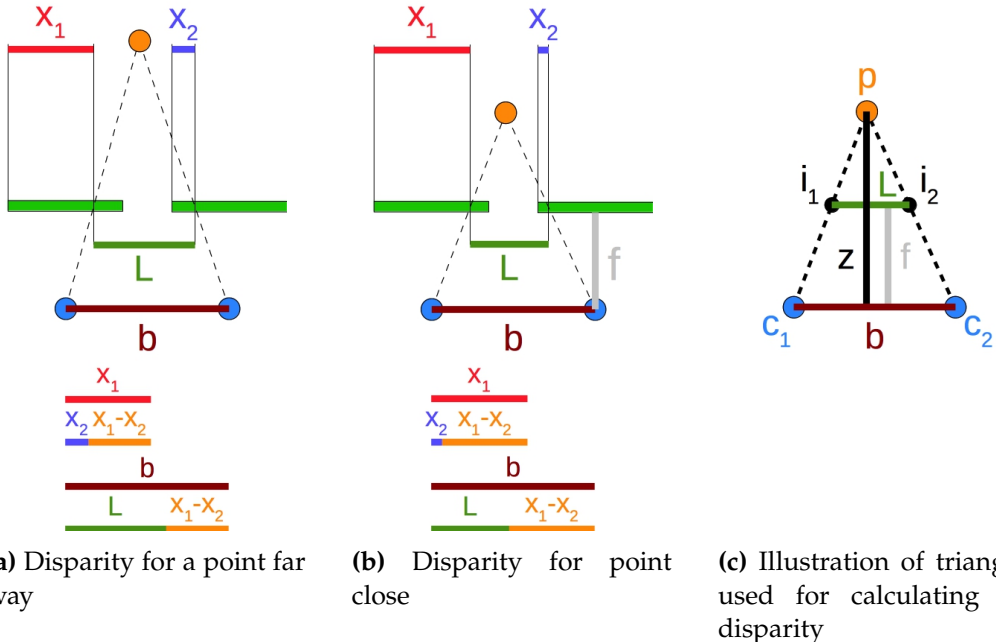


Figure 2.4: Illustration of how to calculate depth from disparity

This explains the basic of stereo vision. The rest of this chapter will venture into other areas of stereo and describe the difficulties and solutions for each area.

2.2 Epipolar Geometry

Section 2.1 assumes that the stereo image planes are ideal, align exactly and being parallel with the baseline but in a real scenario the cameras will have small imperfections and variations which will make the image planes not align perfectly.

Figure 2.5 shows a pair of stereo images. As seen when searching for a corresponding point in the second camera (e.g. the top of the bottle) then a 2D search area is needed. To simplify the search epipolar geometry can be used.

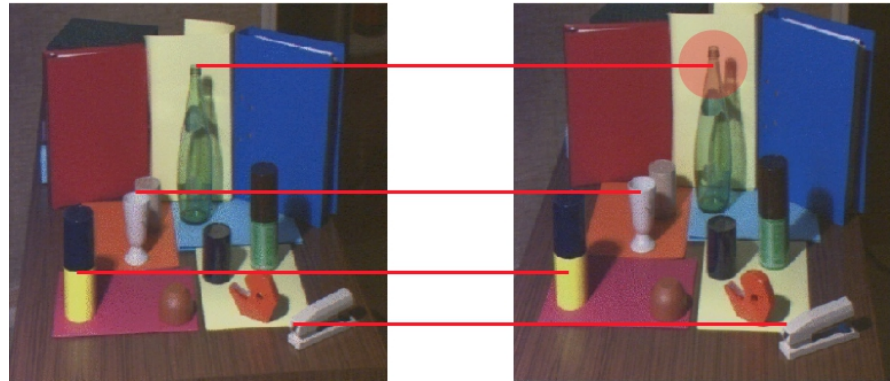


Figure 2.5: Non-rectified stereo pair [4]

Epipolar geometry occurs when a scene is seen from two different views. Figure 2.6 on the facing page illustrates epipolar geometry. An epipole is the projection, on one cameras image plane, of the optical center of the other camera and is illustrated on figure 2.6 on the next page as e_1 and e_2 . The red line going through p_1 (the projection of point P on the image plane) and e_1 is called an epipolar line and a corresponding epipolar line can be found on the other image plane going through p_2 and e_2 . When searching for the corresponding point in the other image the search can be simplified from a 2D search to a 1D search along the epipolar. To simplify the search further, the image can be rectified.

Rectification will transform the stereo images to remove lens distortion and make them into standard form. The standard form is helpful since all epipolar lines then will be horizontal and this simplifies the search for corresponding points to search along the x-axis. Figure 2.7 on the facing page shows the stereo image pair from figure 2.5 but rectified. As seen, now the corresponding points can be found by following the horizontal lines or the x-axis.

The issue with rectification is that it is difficult to get a perfect match with the

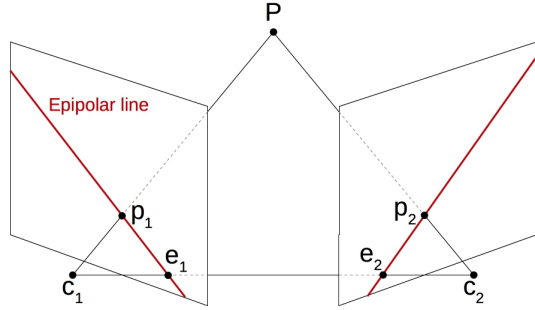


Figure 2.6: Illustration of epipolar geometry

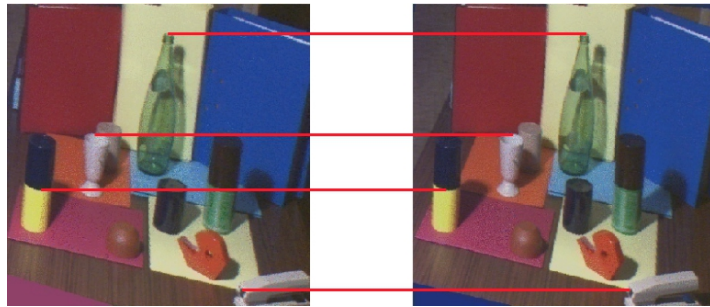


Figure 2.7: Rectified stereo pair [4]

stereo setup since the every camera and its objective will be unique and require and all new manual adjustment. HSA system theorizes that a system can be developed which instead of rectifying the image it will find the epipolar lines and feed this information to the stereo cameras.

In this project stereo image pairs from Middlebury Vision Test sets [5] will be used which are rectified hence the rectification of image will not be researched further in this project.

2.3 Color space and grayscale

Colors can be represented in many different ways digitally using color spaces. Two of the most common color spaces are grayscale and RGB. Some articles have researched what impact different color spaces can have on the result from a stereo algorithm.

For this project the impact of color spaces haven't been studied but instead the findings in [1] are used. This article studies the impact of color spaces on stereo matching by investigating 9 color spaces and 3 different methods. Table 2.1 on the following page shows parts of the results from [1]. In this table the *Measure* column

Measure	Type	Correct [%]	Time
Ncc	G	52.3	52
	C	55.2	141
D ₁	G	49.5	63
	C	51.6	140
PRATT	G	29.1	86
	C	45.2	225
ISC	G	44.9	126
	C	52.6	245
SMPD ₂	G	49.9	569
	C	56.5	2109

Table 2.1: Part of table containing results from [1]

is the algorithm used, *Type* specifies whether it is grayscale (G) or color (C) with the best color space used, the *Correct* column is the percentage of correct matches and *Time* is the execution time. The article concludes that using color always results in better matching but from table 2.1 it is noticed that using grayscale lowers the execution time a lot (down to 27-51 % of color execution time) and in most cases not resulting much worse matching results.

Since the project mostly focuses on a fast stereo matching algorithm and minding the results from table 2.1 it is decided to use grayscale images in case Normalized Cross Correlation is used or to check whether grayscale images gives a much worse result of another algorithm.

2.4 Disparity precision

The depth resolution depends on different things in the stereo camera setup. The camera resolution, the focal length, the baseline etc. HSA system requires that the system have a ≤ 2 mm depth resolution between 0.5 m and 1.5 m.

For a camera HSA systems have a *Imaging Source DMK 72BUC02* available for a stereo camera prototype and the specifications from this camera will be used for the calculations in this section. The camera has a resolution of 2592×1944 and a pixel size of $2.2 \mu\text{m}$. It should also be noted that this camera is monochrome and only have a frame rate of 6 fps hence it cannot be used for a final prototype but these specifications are still used since the camera is available at HSA system and The Imaging Source have similar cameras with higher frame rate and with color. More specifications for the camera can be found at [6]. A baseline of 125 mm is

chosen since HSA system has a simple stereo camera prototype with a baseline of 125 mm.

To calculate the precision equation 2.2 on page 7 is used. This equation is repeated here:

$$z = \frac{b \cdot f}{d} \quad (2.3)$$

An issue with 2.3 is that the disparity, d , is expressed in pixels but to convert it to mm the pixel size of the camera can be used. The lens of the camera can be changed and HSA system has some different lenses with different focal lengths and these are: 6, 9, 16, 25, and 50 mm. Figure 2.8 shows a plot of disparity precision at around 1500 mm distance from the cameras using the camera mentioned and a baseline of 125 mm. The red dots shows the result for the focal length available at HSA system. The green line and red line shows when 4 mm precision and 2 mm precision is achieved. The reason for 4 mm precision is shown is because this can be improved to 2 mm precision using subpixel refinement.

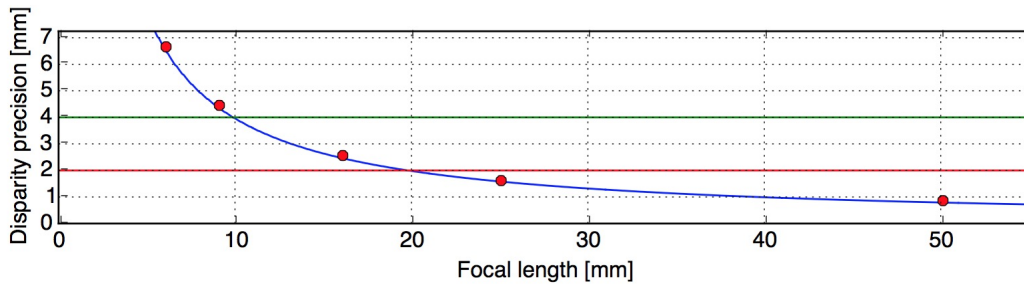


Figure 2.8: Disparity precision at $z \approx 1500$ mm compared to focal length with baseline = 125 mm and using *Imaging Source DMK 72BUC02*

To calculate the disparity precision the disparity value for a distance, z , of at least 1500 mm should be found. Equation ?? on page ?? can be rearranged and pixel size, p_{size} , can be added to calculate a disparity value for a specific distance:

$$d = \frac{b \cdot f}{p_{size} \cdot z} \quad (2.4)$$

The disparity value found by equation 2.4 might not be a integer which the disparity always will be hence the value should be rounded down to ensure an valid value which results in a distance of at least 1500 mm. Adding the known values the following equation is acquired:

$$d_{1500mm} = \left\lfloor \frac{125 \cdot f}{0.0022 \cdot 1500} \right\rfloor \quad (2.5)$$

Then precision at ≈ 1500 mm can be found by using equation 2.3 on the preceding page with disparity, d_{1500mm} , and subtract the distance for disparity, $d_{1500mm} + 1$:

$$d_p = z_{d_{1500mm}} - z_{d_{1500mm}+1} \quad (2.6)$$

$$d_p = \frac{b \cdot f}{p_{size} \cdot d_{1500mm}} - \frac{b \cdot f}{p_{size} \cdot (d_{1500mm} + 1)} \quad (2.7)$$

Equation 2.7 have been used for the plot in figure 2.8 on the preceding page. From the figure it is noticed that 4 mm precision achieved at a focal length of ≈ 10 mm and 2 mm precision achieved at a focal length of ≈ 20 mm. From this a higher focal length is wanted but a higher focal length have a bad influence on scene width and disparity range.

Figure 2.9 shows how focal length influences the scene width. It is noticed that a higher focal length results in a smaller scene hence it is wanted to have a small focal length.

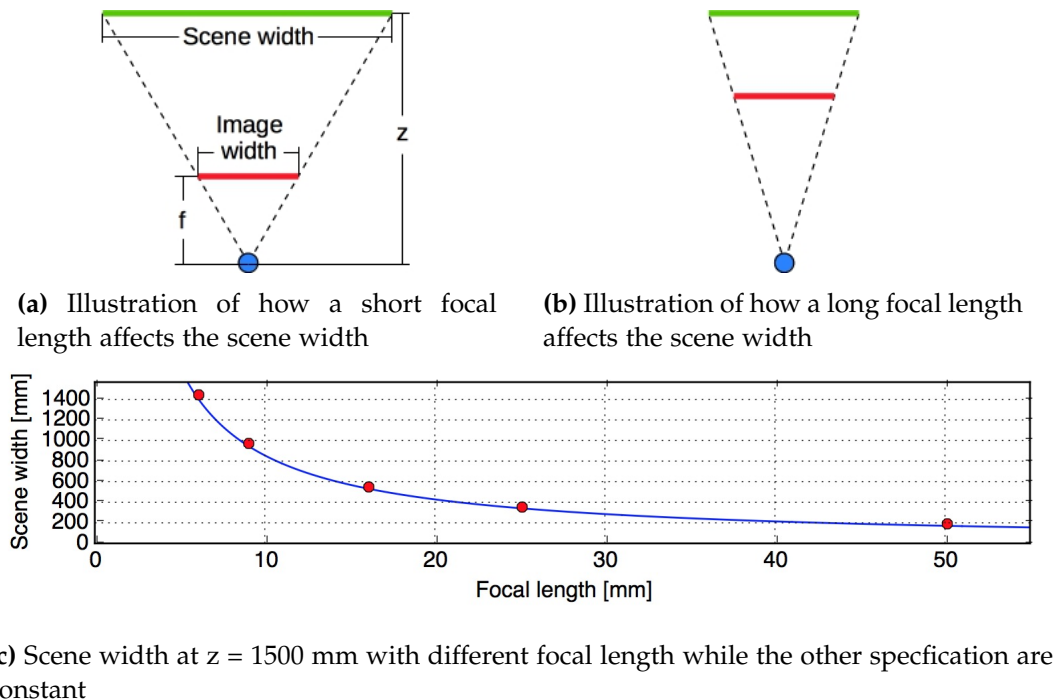


Figure 2.9: Illustration of how focal length affects the scene width at $z = 1500$ mm

Figure 2.10 on the facing page shows the disparity value at maximum distance ($z \approx 1500$ mm), the disparity value at minimum distance ($z \approx 500$ mm) and the range between these two values. As seen the disparity range increases linear with the focal length which results in a large search area hence a lower focal length is wanted.

Using a camera with the same pixel size and resolution as *Imaging Source DMK*

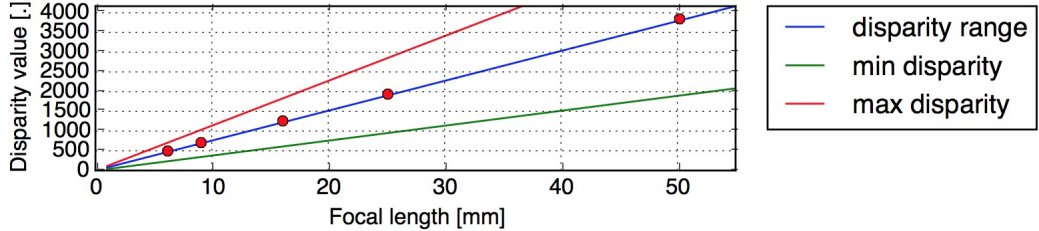


Figure 2.10: Graph of disparity values at minimum distance and maximum distance and the disparity range

72BUC02 a lens with a focal length of 10 mm is wanted while also using subpixel refinement or a lens with a focal length of 20 mm is wanted if subpixel refinement is not being used.

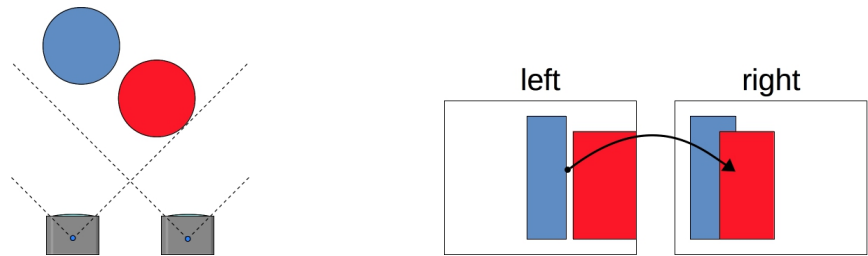
A 10 mm focal length will result in a scene width of 855 mm, a disparity range of 759 and a precision of 3.97 mm. A 20 mm focal length will result in a scene width of 428 mm, a disparity range of 1516 and a precision of 1.98 mm.

Since a disparity range of 1516 is high and a scene width of 428 mm is very small then a 10 mm lens should use together with subpixel refinement.

2.5 Occlusions

Occlusions occur when an object closer to the camera setup blocks some of an object or a whole object behind it. Figure 2.11 illustrates two cylinders seen by a stereo camera setup where occlusion occurs. Figure 2.11a on the next page shows that the right camera can't see all of the blue cylinder because the red cylinder blocks the view while the left camera can see the whole of both cylinder. When searching for corresponding points in the occluded area issues occurs. Following the arrow on figure 2.11b on the following page it is seen that the edge of the blue cylinder can't be found and it will result in calculating a wrong disparity value.

There exist different types of occlusions: partial occlusions, self-occlusions, border occlusions and total occlusions. Partial occlusions are when an object is only partially obstructed as seen on figure ?? on page ???. Self-occlusion occurs on round surfaces such as faces, and balls and as seen on figure 2.12a on the following page the surfaces marked with red can be seen by one camera but not the other camera. Border occlusions occur when an object or part of an object is outside the view of one camera but not the other camera as seen with the blue object on figure 2.12b.



(a) Stereo camera setup with two cylinders in the scene seen from above (b) Image seen by each camera in figure 2.11a

Figure 2.11: Illustration of occlusions

Total occlusion is when an object is completely blocked by an object in the view of one camera but not in the view of the other camera and an example of this is seen with the red object on figure 2.12b.



(a) Illustration of self occlusion seen from above (b) Illustration of total and border occlusions seen from above

Figure 2.12: Illustration of different types of occlusions

Occluded points can be found by running stereo matching again but switching which camera is used as the reference and then compare the disparity values found for each direction. When occluded areas are found these can be filled using different methods. For this project, new methods haven't been developed or studied but instead the findings from [3] is used which will be described in section 2.5.1 to 2.5.4 on pages 14–17. All these methods assume that the stereo matching is using the left image as reference i.e. the points in the left image are searched for in the right image.

2.5.1 Neighbor's Disparity Assignment (NDA)

This is one of the simpler methods to fill occlusions. It functions by selecting an occluded point, p_L , then finds then nearest non-occluded point, q_L , to the left when filling non-border occlusion. With border occlusion, the nearest point to the right is found instead. This method assumes that this non-occluded point is part of the same surface as the occluded point (this can be seen on figure 2.11) and the

disparity value from q_L can be assigned to p_L . This method has some issues. In cases of total occlusions (see figure 2.12b) wrong disparity values will be given to the total occluded object since it isn't a part of the nearest surface with non-occluded points to the left. In cases with self-occlusions the occluded area should have disparity values close to the disparity values of the non-occluded points to the right (This will be the area of the surface which is in view of both cameras) but using NDA will give the occluded area disparity values corresponding to the background.

2.5.2 Diffusion in Intensity Space (DIS)

This method is inspired by diffusion. Diffusion is the movement of molecules or atoms from a high concentration region to a low concentration region.

After detecting occluded regions with cross-checking during stereo matching, the diffusion energy for the region is approximated. This method is depended on the stereo matching algorithm because it uses the energy from the last iteration to determine initial diffusion energy for the area. But a change to the method can be made to make it independent from the stereo matching. The initial energy will be 0. Then the diffusion energy for non-border occlusion is found by:

$$E(p_L) = \min_{l_{p_L}=\{0, \dots, l_{max}\}} \left(\frac{1}{2|q_L \in \mathcal{N}(p_L) \wedge l_{q_L}=l_{p_L}|} \sum_{q_L \in \mathcal{N}(p_L) \wedge l_{q_L}=l_{p_L}} (|\bar{I}(p_L) - \bar{I}(q_L)| + E(q_L)) \right) \quad (2.8)$$

And the diffusion energy for border occlusions are found by:

$$E(p_L) = \min_{l_{p_L}=\{0, \dots, l_{p_{Lf}}-2\}} \left(\frac{1}{2|q_L \in \mathcal{N}(p_L) \wedge l_{q_L}=l_{p_L}|} \sum_{q_L \in \mathcal{N}(p_L) \wedge l_{q_L}=l_{p_L}} (|\bar{I}(p_L) - \bar{I}(q_L)| + E(q_L)) \right) \quad (2.9)$$

The diffusion energy will be calculated for each occluded point and for each point the disparity which corresponds the minimum $E(p_L)$ is set as the disparity l_{p_L} for the occluded point.

2.5.3 Weighted Least Squares (WLS)

In this method, all the non-occluded and filled occluded neighbors in a neighborhood around the occluded point is considered valid points and is used as control points in interpolation.

Since the neighborhood contains both foreground points and background points and the occluded point is expected to be a part of the background then the background points should have higher influence than foreground points. It is assumed

that the color intensity between objects is significantly different and this property can be used to distinguish between foreground points and background points.

Each error term in the aggregated residual should be weighted so the foreground doesn't have much influence. The aggregated residual is then defined as:

$$\Delta = \sum_{q_L \in \mathcal{N}(p_L)} w_{q_L} (\hat{l}_{p_L}(p_L) - l_{p_L}(q_L))^2 \quad (2.10)$$

where $w_{q_L} = e^{-\mu_L |\bar{I}(p_L) - I(q_L)|}$ (the weight) is the likelihood of p_L with q_L under the assumption of an exponential distribution model of $|\bar{I}(p_L) - I(q_L)|$. $\bar{I}(p_L)$ is the mean intensity of p_L and μ_L and is also called the decay rate. $\hat{l}_{p_L}(p_L)$ is the estimated disparity of p_L (will be estimated during interpolation) and $l_{p_L}(q_L)$ is the disparity of q_L .

$\bar{I}(p_L)$ is the mean intensity of p_L which can be obtained using mean shift algorithm in a window around p_L . To estimate this value then initialize the algorithm with $\bar{I}(p_L)$ equal to the intensity of p_L then the mean shift algorithm repeatedly picks those neighbors inside the window that satisfy $|\bar{I}(p_L) - I(q_L)| \geq 3\mu^{-1}$ and the assign the average of intensities of the selected neighbors to $\bar{I}(p_L)$ until $\bar{I}(p_L)$ converges to a fixed average. $|\bar{I}(p_L) - I(q_L)|$ has decay rate μ_L which is related to the decay rate μ of the variable $|I(p_L) - I(q_L)|$ by $\mu_L^2 = \mu$.

For this model a matrix containing the coordinates for all the control points is generated:

$$F = \begin{bmatrix} x_1 & y_1 & 1 \\ \vdots & \ddots & \vdots \\ x_n & y_n & 1 \end{bmatrix} \quad (2.11)$$

and a vector with the corresponding labels for the coordinates in F is generated:

$$L = [l_1 \ \cdots \ l_N] \quad (2.12)$$

Then a Linear model can be expressed as:

$$l_{p_L} = a + bx(p_L) + cy(p_L) \quad (2.13)$$

Where $(x(p_L), y(p_L))$ is the coordinates of p_L and a, b and c are the model parameters.

The weights for the control points can be express in a vector as:

$$w = [w_{q_{L1}} \ w_{q_{L2}} \ \cdots \ w_{q_{LN}}]' \quad (2.14)$$

Then we compute two new matrices, F_w and L_w :

$$F_w = \text{diag}(w)F \quad (2.15)$$

$$L_w = \text{diga}(w)L \quad (2.16)$$

The model parameter vector:

$$P = [a \ b \ c]' \quad (2.17)$$

By combining the equations above then the following equation is given:

$$P = (F_w^T F_w)^{-1} F_w^T L_w \quad (2.18)$$

With these equation the disparity of the occluded point can be estimated:

$$\hat{l}_{p_L} = [1 \ x(p_L) \ y(p_L)]P \quad (2.19)$$

2.5.4 Segmentation-based Least Squares (SLS)

The biggest difference between WLS and SLS is that SLS only uses non-occluded points as control points. The control points is a subset of the non-occluded neighboring points. The control points are segmented from the neighborhood by applying different constraints: visibility constraint, disparity gradient constraint, and color similarity cues. This description of the method will in this report be simple. For a more thoroughly description refer to [3].

First find occluded points which have at least one non-occluded neighboring point. Then these points are sorted by a priority which is found by checking the homogeneity i.e color similarity between the occluded point, p_L and the neighboring non-occluded points. In this case, equation 2.20 can be used to find the homogeneity. The lower result given by the equation the higher the homogeneity is.

$$\sum_{q_L \in N(p_L)} = \psi(p_L, q_L) \quad (2.20)$$

Where q_L is a non-occluded point, $N(p_L)$ is a set of neighboring non-occluded points and $\psi(p_L, q_L)$ is a cut-off function expressed as:

$$\psi(p_L, q_L) = \begin{cases} |\bar{I}(p_L) - I(q_L)| & , \text{ if } |\bar{I}(p_L) - I(q_L)| \leq 3\mu_L^{-1} \\ 3\mu_L^{-1} & , \text{ otherwise} \end{cases} \quad (2.21)$$

When the occluded point with highest priority is found then some initial control points from $N(p_L)$ are needed. First only points from the background is wanted therefore only points in $N(p_L)$ which satisfies $l_{q_L} < l_{p_{Lf}}$ where l_{q_L} is the disparity of a point, q_L in $N(p_L)$ and $l_{p_{Lf}}$ is the disparity of the nearest point from the foreground which is expected to be the nearest non-occluded point to the right

of p_L . But a narrow object in the scene might result in the nearest non-occluded point to the right to be a part of the background therefore a second constraint is added. The nearest non-occluded point to the left is assumed to be a part of the background and therefore all points in $N(p_L)$ which satisfies $|l_{p_{Lb}} - l_{q_L}| \leq 1$ should also be part of the background. $l_{p_{Lb}}$ is the disparity of the nearest non-occluded point to the left. With these constraints a combined constraint can be expressed:

$$|l_{p_{Lb}} - l_{q_L}| \leq 1 \vee l_{q_L} < l_{p_{Lf}} \quad (2.22)$$

All points in $N(p_L)$, which satisfies this combined constraint, is assumed to be part of the background but might contain points from multiple background surfaces. It is assumed, from looking at the data sets from [5], that $N(p_L)$ only contains points from either one background surface or two background surfaces.

First it is needed to calculate whether the points in the updated $N(p_L)$ belongs to one or two surfaces and for this the $l_{max} - l_{min} \leq 1$ can be used. l_{max} is the maximum disparity in $N(p_L)$ and l_{min} is the minimum disparity and if these disparities are close it is assumed that they belong to the same surface and all points in $N(p_L)$ can be used as control points for finding the disparity for p_L . If $l_{max} - l_{min} > 1$ then $N(p_L)$ should be divided into two sets, $N_1(p_L)$ and $N_2(p_L)$.

If a point q_L in $N(p_L)$ satisfies $|l_{max} - l_{q_L}| \leq 1$ then it belongs to $N_1(p_L)$ or if it satisfies $|l_{min} - l_{q_L}| \leq 1$ then it belongs to $N_2(p_L)$. With $N(p_L)$ divided into two groups it is needed to determine which set p_L belongs to. For this the average truncated color distance is used and it is expressed as:

$$D(p_L, N_i(p_L)) = \frac{1}{|N_i(p_L)|} \sum_{q_L \in N(p_L)} \psi(p_L, q_L) \quad (2.23)$$

If $D(p_L, N_1(p_L)) < D(p_L, N_2(p_L))$ then p_L belongs to $N_1(p_L)$ else it belongs to $N_2(p_L)$. Then the set, which p_L belongs to can be used as control points for finding the disparity of p_L .

2.6 Occlusions filling result

In [3] it is found that SLS gives the best result followed by DIS, NDA, and WLS but the runtime SLS is slower than NDA and WLS and faster than DIS. Since the project focuses on implementing a fast stereo algorithm and focuses more on the stereo algorithm itself, NDA is chosen as the method to fill occlusions since it is the better performing of the two faster methods.

2.7 Mini-conclusion

To conclude this chapter the findings for each area in stereo vision will be examined and it will be specified which solution will be used from this point.

Rectification of Images

This project will not delve further into the subject of rectification and data sets from [5], which already is rectified, will be used in this project.

Color Space

The result from [1] shows that color spaces in most cases is a bit better than using grayscale images but the run time is much higher. This result depends on the algorithm used therefore when an algorithm have been chosen a test should check if grayscale images perform much worse than using color images and what the impact to run time is.

Resolution and Disparity Precision

To have a disparity precision of 2 mm at 1500 mm using *Imaging Source DMK 72BUC02* cameras with a resolution of 2592×1944 and a pixel size of $2.2 \mu\text{m}$ a lens with a focal length of 10 mm should be used together with subpixel refinement.

Occlusions

4 different methods to fill occlusions where described and from these NDA is chosen since it is the better performing of the two faster algorithms.

Chapter 3

Requirements

This chapter will contain the requirements for the system and a test specification which will describe how to test for the requirements.

3.1 Requirement specification

No.	Parameter	Value	Unit	Additional Information	Informa-	Source
1	Frame rate	≥ 10	fps			Section 1.2 on page 2
2	Disparity precision	≤ 2	mm	• Either directly or using subpixel refinement		Section 1.2 on page 2
3	Depth range	0.5-1.5	m			Section 1.2 on page 2
4	Camera resolution	2592×1944	pixels			Section 2.4 on page 10
5	Focal length	≥ 10	mm			Section 2.4 on page 10
6	Pixel size	0.0022	μm			Section 2.4 on page 10

General requirements

- For a camera *Imaging Source DMK 72BUC02* or similar camera should be used

3.2 Test specification

This section will describe how to test to ensure requirements are fulfilled.

Requirement 1: frame rate can be tested by running the finalized implementation and measure the run time which then should be \leq .

For requirement 2: disparity precision HSA system produced a test object which has small depth increases. Figure 3.1 shows a 3D model of this test object. This model was 3D printed in case a working prototype of the prototype was available for testing. The steps closest to the bottom right of the figure increase by 1 mm for each step. The next line increase by 2 mm for each step. This continues and the last line of steps increases by 5 mm for each step. The small shapes in the middle of each step have a depth difference of 0.5 mm and alternately protrudes from or recesses into the steps. This object can be used to test where the precision of a stereo setup and algorithm is between 0.5 and 5 mm depending on which lines of step can be seen.

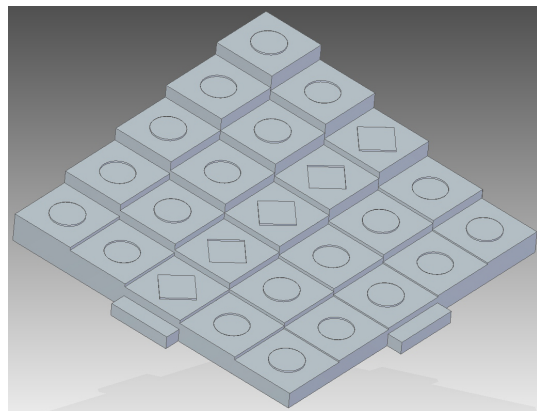


Figure 3.1: 3D model of test object for depth precision

The middlebury test set don't contain images where specific areas contain depth increments of 2 mm and therefore these images can't be used for testing this requirement and we are forced to rely on the calculations from section 2.4 on page 10.

Requirement 3: depth range can only be correctly tested for if a working prototype is developed.

Requirement 4: camera resolution, requirement 5: focal length and requirement 6: pixel size are fulfilled by choosing the correct camera hardware but are essential to be fulfilled for requirement 2 to be fulfilled.

Chapter 8 on page 43 will perform the available tests.

Chapter 4

Algorithm design

In this chapter the two stereo vision algorithms, Efficient Edge Preserving Stereo Matching (EEPSM) and Fast Cost-Volume Matching (FCV), is described. Lastly, a simulation of each algorithm is created and the results of these simulations are compared and from this, an algorithm is chosen.

ROUGH SKETCH not done yet

4.1 Efficient Edge Preserving Stereo Matching:

This algorithm works in three steps. The first step is calculating a cost for each pixel and disparity. This cost is a combination of the sum of absolute differences and hamming distance of the census transform around each pixel.

$$C_d^{SAD}(x, y) = \sum_{i=1}^3 |I_{left}(x, y, i) - I_{right}(x + d, y, i)| \quad (4.1)$$

$$C_d^{CENSUS}(x, y) = Ham(CT_{left}(x, y), CT_{right}(x + d, y)) \quad (4.2)$$

$$C_d(x, y) = \alpha \cdot C_d^{SAD}(x, y) + (1 - \alpha) \cdot C_d^{CENSUS}(x, y) \quad (4.3)$$

where d is the disparity estimate, I_{left} is the left image, I_{right} is the right image, i is the color (rgb), $Ham(x_1, x_2)$ is the hamming distance between x_1 and x_2 , and CT_{left} and CT_{right} is the census transform around the specified pixel

then a permeability weight is calculated. Permeability is known from biomedicine and describes the ability to transfer through a membrane. The permeability weight is inspired by this and describes how well the color transfers from one pixel to another pixel.

$$\mu(x, y) = \min(e^{\frac{-\Delta R}{\sigma}}, e^{\frac{-\Delta G}{\sigma}}, e^{\frac{-\Delta B}{\sigma}}) \quad (4.4)$$

$$\mu_{tb}(x, y) = \min(e^{\frac{-(R(x,y)-R(x,y-1))}{\sigma}}, e^{\frac{-(G(x,y)-G(x,y-1))}{\sigma}}, e^{\frac{-(B(x,y)-B(x,y-1))}{\sigma}}) \quad (4.5)$$

lastly, the cost is aggregated resulting in a combined cost for each pixel at each disparity. The cost from equation ?? is first aggregated horizontally using permeability weights from equation ???. Then the result from horizontal aggregation is aggregated vertically also using the permeability weight.

$$C_d^{lr}(x, y) = C_d(x, y) + \mu_{lr}(x, y) \cdot C_d(x - 1, y) \quad (4.6)$$

$$C_d^{lr}(x, y) = C_d(x, y) + \sum_{i=1}^{x-1} \left(C_d(x - i, y) \cdot \prod_{j=i}^x \mu_{lr}(x - j, y) \right) \quad (4.7)$$

With a cost at each pixel at each disparity estimate, the disparity map can be generated by minimization along the disparity estimates.

4.2 Fast Cost-Volume Matching:

This algorithm starts by calculating a cost for each pixel at each disparity estimate. This cost consists of the sum of absolute differences and differences in the gradient.

$$C_d^{SAD}(x, y) = \sum_{i=1}^3 |I_{left}(x, y, i) - I_{right}(x + d, y, i)| \quad (4.8)$$

$$C_d^{Grad}(x, y) = \nabla_x I_{left}^g(x, y) - \nabla_x I_{right}^g(x, y) \quad (4.9)$$

$$C_d(x, y) = \alpha \cdot C_d^{SAD}(x, y) + (1 - \alpha) \cdot C_d^{Grad}(x, y) \quad (4.10)$$

These cost values are then filtered using a Guided Image Filter. The guided image filter is a filter uses a reference image to generate the weights. The guided image filter is described further in section 4.2.1

$$C'_d(x, y) = \sum_j W_{i,j}(I) C_d(x, y) \quad (4.11)$$

The correct disparity for each pixel can then be found by minimizing along the disparity estimates as seen in equation 4.12.

$$f(x, y) = \arg \min_{d \in [0, d_{max}]} C'_d(x, y) \quad (4.12)$$

4.2.1 Guided image filter

The guided image filter uses a image as a reference for weighting the input. The output from the filter is seen in equation

$$q_i = \sum_j W_{i,j}(I) p_j \quad (4.13)$$

$$q_i = a_k I_i + b_k \quad , \forall i \in \omega_k \quad (4.14)$$

where:

$$a_k = \frac{\frac{1}{|\omega|} \sum_{i \in \omega_k} I_i p_i - \mu_k \bar{p}_k}{\sigma_k^2 + \epsilon} \quad (4.15)$$

$$b_k = \bar{p}_k - a_k \mu_k \quad (4.16)$$

algorithm

Input:

filtering input image: p

guidance image: I

radius: r

epsilon: ϵ

Output:

filtering output: q

Steps:

1. $\mu_I = f_{mean}(I)$
 $\mu_p = f_{mean}(p)$
 $\rho_{II} = f_{mean}(I \cdot I)$
 $\rho_{Ip} = f_{mean}(I \cdot p)$
2. $\sigma_I = \rho_{II} - \mu_I \cdot \mu_I$
 $cov_{Ip} = \rho_{Ip} - \mu_I \cdot \mu_p$
3. $a = cov_{Ip} / (\sigma_I + epsilon)$
 $b = \mu_p - a \cdot \mu_I$
4. $\mu_a = f_{mean}(a)$
 $\mu_b = f_{mean}(b)$
5. $q = \mu_a \cdot I + \mu_b$

4.3 Simulation and comparison

simulation af de 2 algoritmer og sammenligne resultaterne.

4.4 Choosing an algorithm

Nok en anden titel til denne sektion. Skriv hvilken algoritme jeg går videre med

Chapter 5

Platform Analysis

5.1

- beskriv Zynq platformen.
kom ind på hvad den indeholder
- bedre navn og cite ds190
product specification og måske trm?
- FPGA constraints ==> $C = f(A, T, P, N)$, Lav en tabel

Part	Quantity
Programmable logic cells	85,000
Look-Up Tables	53,200
Flip-flops	106,400
Extensible Block Ram	560 kB
Programmable DSP slices	220

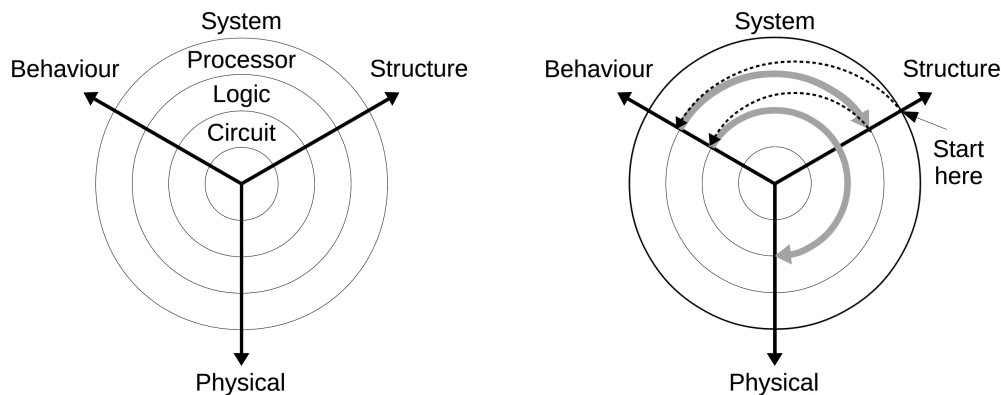
Table 5.1: Parts on zynq 7020

Chapter 6

Design methodology

In [2] the Gajski-Kuhn Y-chart is described and it is illustrated on figure 6.1a. This chart can help describe a way to design a system. It moves between the three domains: Behaviour, Structure and Physical.

læs om system design methodologies i gajski's **Embedded Systems Design - Modeling, Synthesis and Verification** og beskriv Platform Methodology



(a) Illustration of the standard Gajski-Kuhn Y-chart [2]

(b) Illustration of the Gajski-Kuhn Y-chart showing the FPGA methodology [2]

Figure 6.1: Illustrations of Gajski-Kuhn Y-chart

noter til mig selv

- processor synthesis:
 - side 32 i gajski pdf
 - (a) allocation of components and connections
 - (b) cycle-accurate scheduling
 - (c) Binding of variables, operations and transfers
 - (d) Synthesis of controller

(e) Model refinement

(a-c) kan udføres sammen eller i hvilken som helst rækkefølge men de er afhængige af hinanden. Hvis de udføres samtidigt bliver synthesen kompleks og utilregnelig. en strategi er at udføre det i følgende rækkefølge: a c b

Alle trinene ovenover kan udføres automatisk eller manuelt. Hvis det hele bliver udført automatisk kaldes det processor-level synthesis eller high-level synthesis (HLS). Hvis a-d blvver udført manuelt og e automatisk kaldes det model refinement.

System-level behavioral model / system synthesis: side 35

- (a) Profiling and estimation.
- (b) Component and connection allocation
- (c) Process and channel binding
- (d) Process scheduling
- (e) IF component insertion
- (f) Model refinement

1.3 System Design methodology: side 39

model algebra side 42

algebra:<objects, operations>

$$a * (b + c) = a * b + a * c$$

dette gør det muligt for system designere at optimere designet vha. arithmetic algebra regler. Udtrykket til venstre for = kræver en multiplicer og en adder hvorimod udtrykket på højre side kræver 2 multipliers og en adder.

modelalgebra : <objects, compositions>

1.4 System-level models: side 44

applications designers, system designers og implementations designers.

2 system design methodologies side 56

Dette kapitel beskriver forskellige system design methodologies.

Bottom-up: start i bunden (circuit level) kør fra behavior til physical og lav et library. brug dette library til næste level.

Top-down: Start i øverste level (system level) kør fra behavior over til structure. gå et level ned og gentag. ved nederste level gå fra behavior til physical.

Platform methodology: side 61

FPGA methodology: side 64

er based på FPGA substrat som består af multitude af 4-bits ROM celler (Look-up Tables (LUTs)) og disse LUTs kan implementere enhver 4-variable boolsk funktion. I denne design metodologi vil hver RTL komponent i biblioteket være opbygget af disse 4-variable funktioner. Og derefter bliver processor delene synthesizeret af

disse RTL komponenter.

sagt på en anden måde: denne metodologi bruger en top-down approach på både system og processor levels hvor standard og custom Processing Elements og Communication Elements er opbygget af LUTs. Et system design starter ved at man mapper en applikation ned på en given platform og derefter syntheser brugerdefineret komponenter ned til RTL komponenter som er defineret i form af LUTs. Standard processor komponenter i processor biblioteket er allerede defineret i form af LUTs. Når alle vores komponenter er defineret vha LUTs så simplificere vi designet ned til LUTs og BRAM og derefter kan vi udføre placering og routing med værktøjer FPGA producentet har udviklet.

Denne form for top-down metode har de samme svagheder som andre top-down metoder som er at det kan være svært at optimere hele designet ved at simplificere designet ned til basiske LUT celler. Derudover ved udvikler heller ikke om hvordan FPGA producentens værktøj placerere og forbinder LUTs og BRAMs.

Chapter 7

Architecture design

This chapter will describe the design process for the hardware architecture. In section ?? a parallelism analysis is performed. Section ?? will describe the allocation and scheduling of the hardware elements.

NOT DONE! rough sketch. De nedenstående trin er hvad jeg skal igennem: Para. Anal., Alloc., Optimizaiton, FSMD og VHDL + simulering

7.1 Parallelism Analysis

The inherent parallelism of the system has been analyzed to find out which improvements can be made. Figure xx shows a diagram of the whole system and on the following pages, data flow graphs (DFG) for each subsystem can be found.

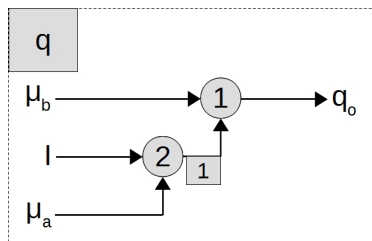


Figure 7.1: Synchronous data flow graph of the q block in the guided image filter

To find the parallelism in the system precedence graphs (PG) have to be created. Since the subsystems are simple the precedence graphs can be created looking at the system from end to start and for each operator find out which signal is needed and have to be calculated before. Another method is to create a synchronous data flow graph (SDFG) and from the SDFG a matrix, $\underline{\underline{L}}$ can be created. This matrix expresses the relationship between the in- and outputs from each node in the SDFG and is called the *topology* matrix. An example of an SDFG is illustrated on in figure

7.1. In this example the topology matrix is then:

$$\underline{\Gamma} = \begin{matrix} & \text{nodes} \\ \text{arcs} & \begin{bmatrix} -1 & 1 \end{bmatrix} \end{matrix} \quad (7.1)$$

If $\text{rank}(\underline{\Gamma}) \leq s - 1$ where s is the number of nodes then a positive integer vector \underline{q} can be found such that $\underline{\Gamma} \cdot \underline{q} = \underline{0}$. Then resulting \underline{q} is:

$$\underline{q} = \begin{bmatrix} 1 \\ 1 \\ 1 \end{bmatrix} \quad (7.2)$$

This \underline{q} vector expresses how many times each node have to be executed within one sample period.

With $\underline{\Gamma}$ and \underline{q} a periodic admissible sequential sequence (PASS) can be found. This tells a sequential sequence in which the nodes can be executed and with it, a periodic admissible parallel sequence (PAPS) can be generated. To find the PASS generate a randomly ordered list of all the nodes, L . For each

7.2 Allocation and Scheduling

To develop a Finite State Machine (FSM) we need to know which hardware is allocated and when each operation is scheduled. This enables us to define some states for the FSM.

From section 7.1 on the previous page some precedence graphs are found and theses graphs shows how many FUs can run in parallel. We need to know how much hardware is needed for each FU. To calculated some simple system have been generate in Vivado 2016.2 and then synthesized. Then utilization of the hardware can be found. Appendix A on page 49 describes in detail the procedure and table ?? shows the result.

	LUT	FF	BRAM	DSP48
Adder	15	15	-	-
Adder/Subtracter	≈ 16	15	-	-
Subtract	15	15	-	-
Multiplier - LUT	352	36	-	-
Multiplier - DSP48	-	-	-	1
Divider	≈ 177	82	0.5	7

Table 7.1: Number of logic elements used in average for each FU

To create the FSM specification we need to introduce time into the precedence graphs to establish some states. To achieve this scheduling is used. There exists different methods for scheduling and some of these are:

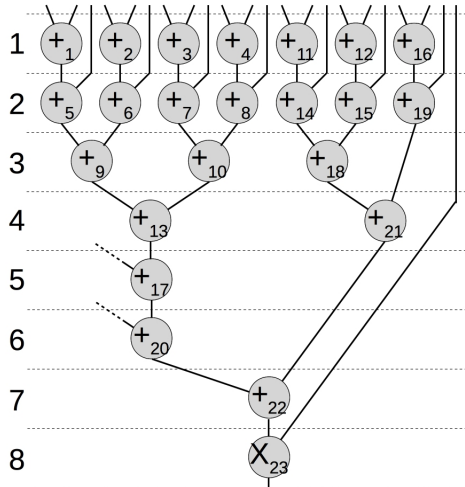
- Resource Constrained (RC)
- Time Constrained (TC)

7.2.1 RC scheduling

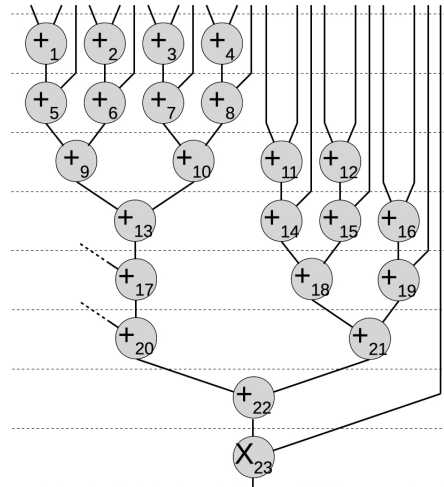
For both methods the first step is create as soon as possible (ASAP) and as late as possible (ALAP) schedules. Then for the RC scheduling a ready list is created. This list contains a list of operations which are ready for scheduling and sorted by mobility. The mobility, $M(op)$, expresses the difference between the states in which the operation, op , have been scheduled in ASAP and ALAP schedules, e.i. $S_{ALAP}(op) - S_{ASAP}(op)$.

lav om til operation og
husk mult

Figure 7.2 shows an example of an ASAP and an ALAP schedule. As seen on the figure node 1-10, 13, 17, 20 and 22-23 are part of the critical path and therefore mobility is 0 for each of the nodes. Nodes 11-12, 14-15, 18 and 21 all have a mobility of 2 and nodes 16 and 19 have a mobility of 3.



(a) Example of ASAP schedule



(b) Example of ALAP schedule

Figure 7.2: Illustration of ASAP and ALAP schedules. The illustration shows a part of the mean filter shown on figure ?? on page ??

With mobility found for each node/operation then a ready list can be generated. Add every ready node and then sort them by mobility. In the start the list would look like this: 1. node 1 ($M(+1) = 0$), 2. node 2 ($M(+2) = 0$), 3. node 3

($M(+_3) = 0$), 4. node 4 ($M(+_4) = 0$), 5. node 11 ($M(+_{11}) = 2$), 6. node 12 ($M(+_{12}) = 2$) and 7. node 16 ($M(+_{16}) = 3$).

Lets say the system have 3 ALU's available then node 1-3 can be scheduled to state 1 since they are higher on the ready list and there is no free ALU for the remaining nodes. The scheduled nodes are removed and the ready list is updated with newly available nodes. The list is still sorted by mobility and will now look like this: 1. node 4 ($M(+_4) = 0$), 2. node 5 ($M(+_5) = 0$), 3. node 6 ($M(+_6) = 0$), 4. node 7 ($M(+_7) = 0$), 5. node 11 ($M(+_{11}) = 2$), 6. node 12 ($M(+_{12}) = 2$) and 7. node 16 ($M(+_{16}) = 3$).

Then nodes 4-6 are scheduled into state 2 since they have lower mobility than the rest of the ready list. The list is updated again and will look like this: 1. node 7 ($M(+_7) = 0$), 2. node 8 ($M(+_8) = 0$), 3. node 9 ($M(+_9) = 0$), 4. node 11 ($M(+_{11}) = 2$), 5. node 12 ($M(+_{12}) = 2$) and 6. node 16 ($M(+_{16}) = 3$).

Nodes 7-9 are scheduled into state 3 and the list is updated again: 1. node 10 ($M(+_{10}) = 0$), 2. node 11 ($M(+_{11}) = 2$), 3. node 12 ($M(+_{12}) = 2$) and 4. node 16 ($M(+_{16}) = 3$).

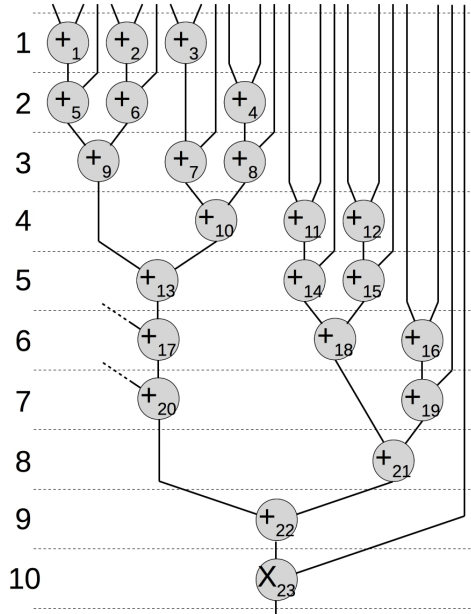


Figure 7.3: RC schedule

This is repeated until all nodes have been scheduled and the result is seen in figure 7.3. This schedule uses 2 states more than the ASAP and ALAP but it

reduces the cost since it uses 1 less ALU than the ALAP schedule and 5 less than the ASAP schedule.

This information is described in [2].

7.2.2 TC schedule

The RC schedule improves the cost of the implementation while the TC intends to improve the performance of the implementation. First a maximum number of states is decided and then ASAP and ALAP schedules are generated and mobility ranges are found. Then some probabilities are assigned to each operation. These probabilities express the probability for the specified operation to be scheduled in each state in its mobility range e.g. operation 11 in 7.2 on page 35 have 1/3 probability for being scheduled in each of state 1-3 if maximum number of states is kept at 8. Figure 7.4 shows the probabilities for each operation in figure 7.2 on page 35. Fortsæt med at skrive senere

		ALU	MULT
1	+ ₁ + ₂ + ₃ + ₄	$1 \times 4 + 1 / 3 \times 2 + 1 / 4 = 4^{11} / _{12}$	0
2	+ ₅ + ₆ + ₇ + ₈	$1 \times 4 + 1 / 3 \times 4 + 1 / 4 \times 2 = 5^{10} / _{12}$	0
3	+ ₉ + ₁₀	$1 \times 2 + 1 / 3 \times 5 + 1 / 4 \times 2 = 4^2 / _{12}$	0
4	+ ₁₃	$1 + 1 / 3 \times 4 + 1 / 4 \times 2 = 2^{10} / _{12}$	0
5	+ ₁₇	$1 + 1 / 3 \times 2 + 1 / 4 \times 1 = 1^{11} / _{12}$	0
6	+ ₂₀	$1 + 1 / 3 = 1^{1} / _{3}$	0
7	+ ₂₂	1	0
8	X ₂₃	0	1

Figure 7.4: Probabilities for each operation in figure 7.2 on page 35

7.3 Finite State Machine with Data Path design

7.3.1 FSMD example

This section will contain an example of a FSMD design example but only of a small part of the system to show how to design a FSMD but also to show that it is a really extensive process. For this example the *b* block (see figure 7.17 on page 42) from the guided image filter (see figure 7.11 on page 41) and it is shown here on figure 7.5a on the following page.

find et bedre ord

tjek op på synkront dataflow diagram og state diagram

tænk i register! transfer! level og ikke i FSMD

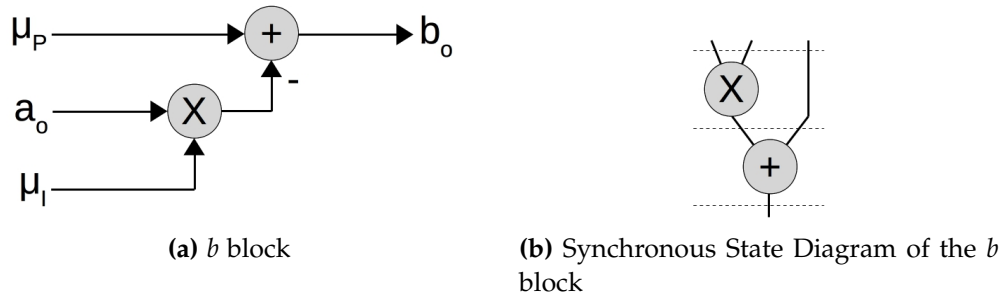


Figure 7.5: b block FSMD stuff

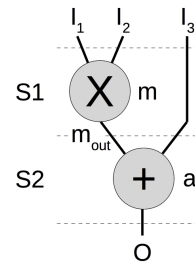


Figure 7.6: Synchronous State Diagram with every connection, functional units, in- and outputs named

	S ₁	S ₂
I ₁	✓	
I ₂	✓	
I ₃		✓
m _{out}		✓
O		✓

Table 7.2: Life-time analysis

```
-- test
...
begin
process (clk) -- Sequential process
begin
  if rising_edge(clk) then
    state <= next_state;
  end if;
end process;

process (state, reset, cars, short, long) -- Combinational process
```

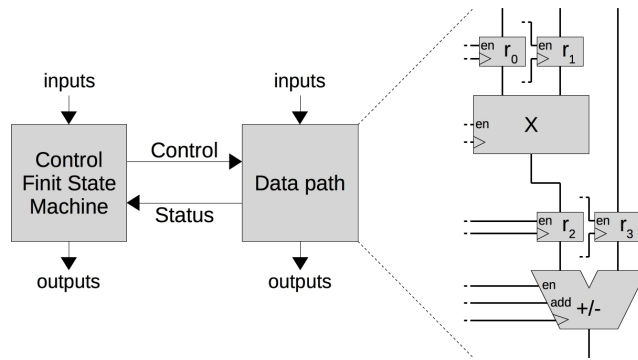


Figure 7.7: Finite State Machine with Data path and the design of the data path is shown.

```

begin
  if reset = '1' then
    next_state <= S1;
  else
    case state is
      when S1 =>
        m_out = I_1 * I_2;
      when S2 =>
        r_2 <= m_out;
        0 <= r_2-I_3;
    end case;
  end if;
end process;

```

noter til mig selv

Controller <-signaler-> Data path

Controller:

Data path: indeholder register, FU, connections, network osv.

skal jeg lave et eksempel med en lille del af mit system? så kan man se hvor voldsomt det kan blive og se processen. Derefter kan jeg vise hvad jeg kommer frem til

noter fra møde med peter:

- lifetime analysis
- synchronous diagram

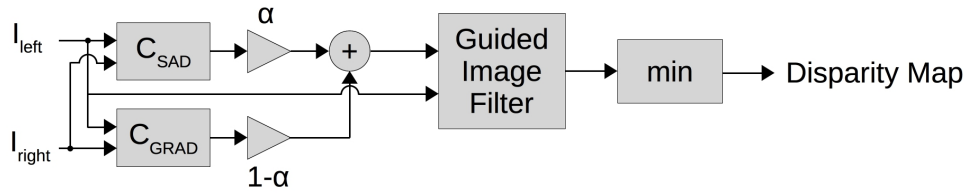


Figure 7.8: Data flow graph of the whole system

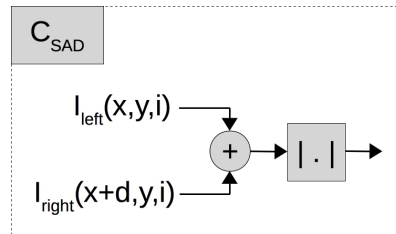


Figure 7.9: Data flow graph of the C_{SAD} block in figure 7.8

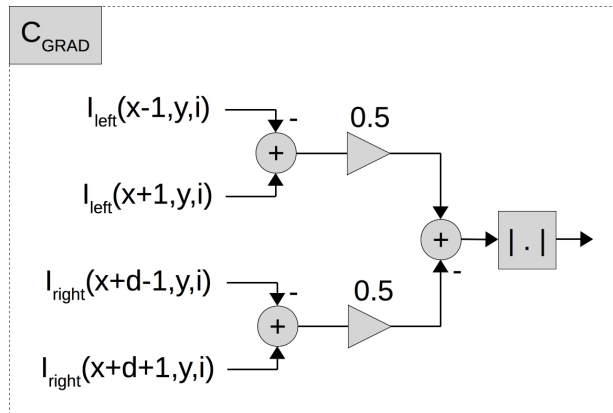


Figure 7.10: C_{GRAD} ikke sikker

noter til mig selv

7.4 VHDL + Simulation

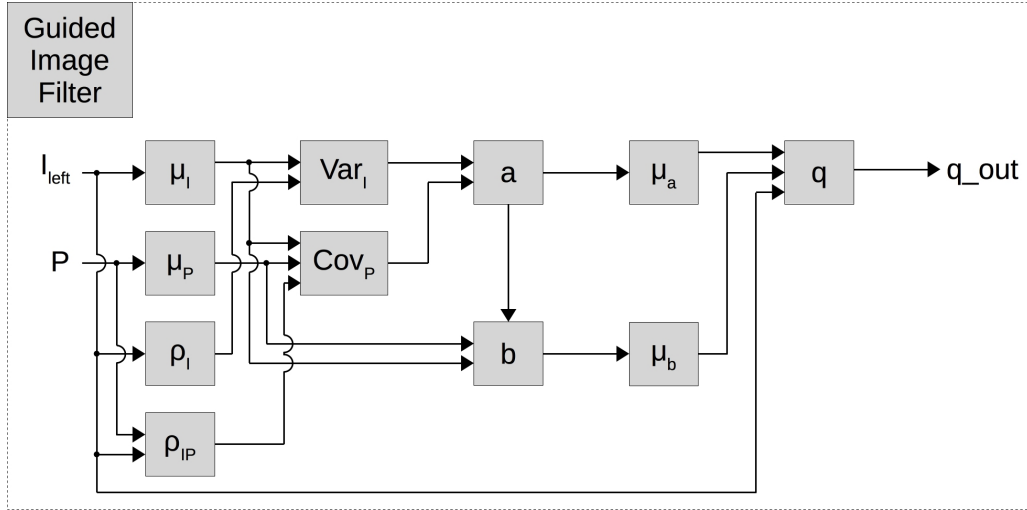


Figure 7.11: Guided image filter

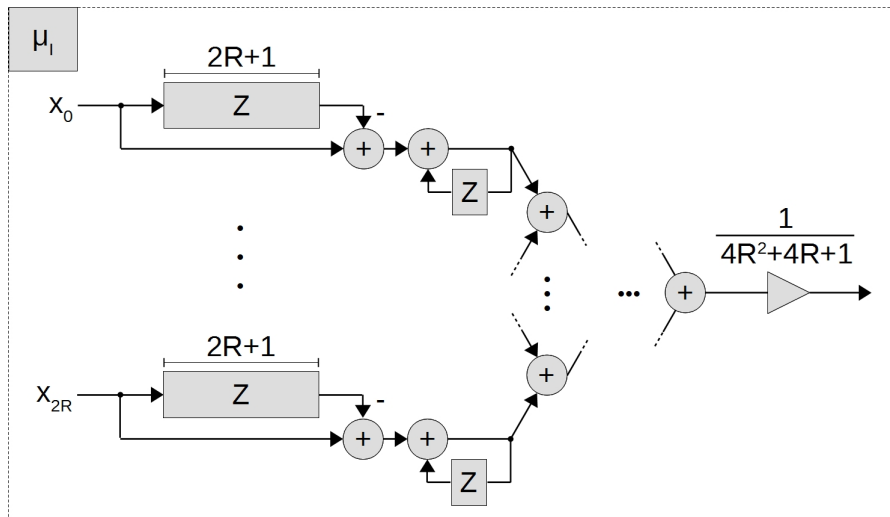


Figure 7.12: Mean filter

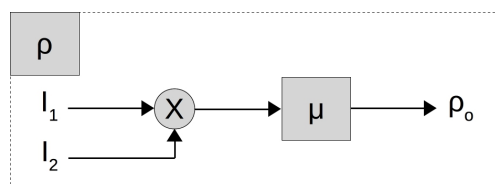


Figure 7.13: Correlation

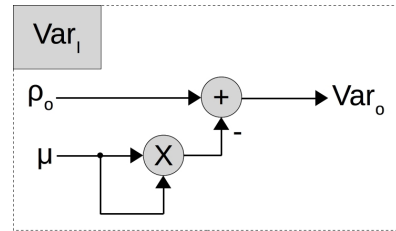


Figure 7.14: Variance

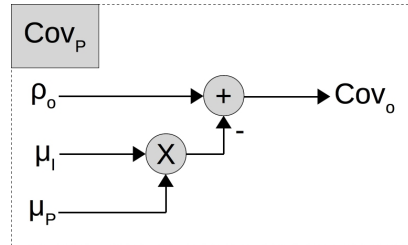


Figure 7.15: Covariance

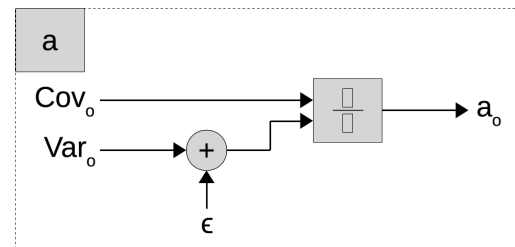


Figure 7.16: A box

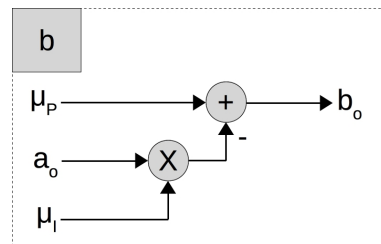


Figure 7.17: B box

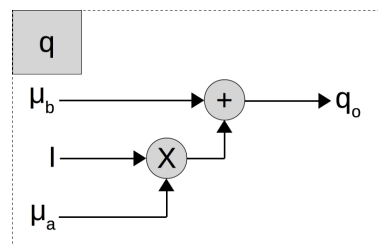


Figure 7.18: Q box

Chapter 8

Acceptance test

udfør accept test udfra
test specifikationen (brug
data fra python simuler-
ing og giv det til VHDL
implementationen)

Chapter 9

Conclusion

This chapter will contain the conclusion

Bibliography

- [1] Sylvie Chambon and Alain Crouzil. "Colour correlation-based matching". In: International Journal of Robotics and Automation 20.2 (2005), pp. 78–85.
- [2] Daniel D. Gajski et al. Embedded System Design - Modeling, Synthesis and Verification. Springer, 2009.
- [3] Shafik Huq, Andreas Koschan, and Mongi Abidi. "Occlusion filling in stereo: Theory and experiments". In: Computer Vision and Image Understanding 117.6 (2013), pp. 688–704.
- [4] Stefano Mattoccia. Stereo Vision: Algorithms and applications. <http://www.vision.deis.unibo.it/smatt/Seminars/StereoVision.pdf>. 2013.
- [5] Daniel Scharstein, Richard Szeliski, and Heiko Hirschmüller. vision.middlebury.edu/stereo. vision.middlebury.edu/stereo. 2016.
- [6] The Imaging Source. DMK 72BUC02 - USB 2.0 monochrome industrial camera. <https://www.theimagingsource.com/products/industrial-cameras/usb-2.0-monochrome/dmk72buc02/>. 2016.
- [7] Richard Szeliski. Computer Vision: Algorithms and Applications. Springer, 2010.
- [8] The Turing Institute. The History of Stereo Photography. http://www.arts.rpi.edu/~ruiz/stereo_history/text/historystereog.html. 1996.

Appendix A

Allocation test

This appendix will explain how the average allocation of logic elements for each functional unit is found.

The result is used in table ?? on page ?? in chapter 7. The table is repeated here in table A.1

	LUT	FF	BRAM	DSP48
Adder	15	15	-	-
Adder/Subtractor	≈ 16	15	-	-
Subtract	15	15	-	-
Multiplier - LUT	352	36	-	-
Multiplier - DSP48	-	-	-	1
Divider	≈ 177	82	0.5	7

Table A.1: Number of logic elements used in average for each FU

A.1 General procedure

This section will describe the general procedure to find the utilization of logic elements for the specified FUs.

First a new project is created in Xilinx Vivado 2016.2. All the settings are set to standard except for the target which is set to ZedBoard Zynq Evaluation and Development Kit. Then a block design is created and a single IP of the wanted type is added. Then for each input and output a port is generated. The inputs are connected to the corresponding ports and between the output of the IP and the corresponding port a Xilinx Slice IP core is inserted which strips every bits except one (MSB) from the output and this IP is connected to the output and the port. This is done to not use to many I/O ports which will make . Using TCL

commands the IP block is copied 99 times and for each copy a new slice and output port is generated and connected to the copy. The inputs are all connected the original corresponding ports except for the divider FU where each copy will have its own input ports. When everything have been connected then Vivado is set to generate top-level HDL wrapper for the block design. Run synthesis and implementation and after completion check the utilization table under the project summary. Note these values, go to the block design and change one of the slices to full output width. Then run synthesis and implementation again and notices if there is a difference in LUT utilization. The LUT utilization is this value minus the LUT value from the former run + 1. These values should be divided by 100 and inserted into table A.1 on the previous page.

The following sections will describe the specific settings for each FUs.

A.2 Adder

This FU uses the Xilinx Adder/Subtracter v12.0 LogiCORE IP. The IP is set to implement using *Fabric*. The inputs are set to a width of 15 bits, mode is set to *add* and the output is set to 15 bits and latency is set to 1. All control signals are disabled.

A.3 Subtract

This FU uses the Xilinx Adder/Subtracter v12.0 LogiCORE IP. The IP is set to implement using *Fabric*. The inputs are set to a width of 15 bits, mode is set to *subtract* and the output is set to 15 bits and latency is set to 1. All control signals are disabled.

A.4 Adder/Subtract

This FU uses the Xilinx Adder/Subtracter v12.0 LogiCORE IP. The IP is set to implement using *Fabric*. The inputs are set to a width of 15 bits, mode is set to *add subtract* and the output is set to 15 bits and latency is set to 1. All control signals beside the ADD signal are disabled.

A.5 Multiplier - LUT

This FU uses the Xilinx Multiplier v12.0 LogiCORE IP. The IP is set to construct the multiplier using *LUTs* and is set to optimize for speed. The inputs are set to a width of 18 bits and the output is set to 36 bits and pipeline stages is set to 1. All control signals are disabled.

A.6 Multiplier - DSP48

This FU uses the Xilinx Multiplier v12.0 LogiCORE IP. The IP is set to construct the multiplier using *Mults* and is set to optimize for speed. The inputs are set to a width of 18 bits and the output is set to 36 bits and pipeline stages is set to 1. All control signals are disabled.

A.7 Divider

This FU uses the Xilinx Divider Generator v5.1 LogiCORE IP. The algorithm type is set to *High Radix*. The inputs are set to a width of 8 bits and the output fractional width is set to 8 bits and latency is set to 3. All control signals are disabled. With this only 5 instances of the Divider is used since each instance uses a lot of IO and to ensure the ability to run implementation without error.

Appendix B

Extra Figures

noter til mig selv

This chapter will contain extra which might fill to much in the report. Looking at you precedence graphs. Maybe make it as fold out image as we did with large diagrams in earlier reports.